without involving the hot-spot spectra. The function fitting also allows them to determine the AF peak position even in the overdoping region where the peak shape is ambiguous due to strong in-gap pristine intensity. They reported the unconventional reconstruction of the Fermi surface, characterized by the coexisting L-circle and pockets, originates from strong correlations instead of static disorder.

Their high-resolution ARPES shows that the nodal quasiparticle spectrum contains both folded AF and unfolded pristine components, consistent with numerical simulations. By monitoring the doping evolution of the folded AF branch, the study finds that superconductivity appears when the folded hole band first crosses the Fermi energy within a short-range AF ground state, near a possible quantum critical point separating static and dynamic AF order. Notably, the zero-energy spectral weight of the hole band scales with T_C, while the energy difference between the band top and the Fermi level is inversely correlated with T_C. These findings indicate that an incipient hole band, driven by electron–spin fluctuation coupling, plays a central role in the emergence of superconductivity in electron-doped cuprates. (Reported by Cheng-Maw Cheng)

This report features the work of Changyoung Kim and his collaborators published in Nat. Commun. ***16****, 2764 (2025).*

TPS 39A Nanometer Angle-resolved Photoemission Spectroscopy (NanoARPES)

- Angle-resolved Photoemission Spectroscopy
- Materials Science, Condensed-matter Physics

Reference

1. D. Song, S. Lee, Z. Shen, W. Jung, W. Lee, S. Choi, W. Kyung, S. Jung, C.-M. Cheng, J. Kwon, S. Ishida, Y. Yoshida, S. R. Park, H. Eisaki, Y. Wang, K.-Y. Choi, C. Kim, Nat. Commun. **16**, 2764 (2025).

Spin-Valley Coupling Enhanced High-T_C Ferromagnetism in a Non-van der Waals Monolayer Cr_2Se_3 on Graphene

Metallic ferromagnetism with a record high Curie temperature (T_C ~225 K) originating from spontaneous spin-valley polarization is reported for a binary monolayer: Cr_2Se_3 on graphene.

Spin-valley coupled magnetic ordering is known to occur in layered van der Waals transition-metal dichalcogenides, but with ordering temperatures below 55 K. Recent theoretical studies predicted that non-van der Waals structures can also exhibit spin-valley polarization–induced semiconducting ferromagnetic (FM) ground states, but experimental confirmation was lacking. In an international collaboration between Japan, France, and Taiwan, researchers have now reported a record high Curie temperature (T_C ~ 225 K) metallic ferromagnetism arising from spontaneous spin-valley polarization in the non-van der Waals monolayer (ML) of the binary compound Cr_2Se_3 on graphene. Using angle-resolved photoemission spectroscopy (ARPES), X-ray absorption spectroscopy (XAS), X-ray magnetic circular dichroism (XMCD), and circular dichroism (CD) in ARPES, Chien-Wen Chuang (Tohoku University), Takafumi Sato (Tohoku University), Ashish Chainani (NSRRC) and their collaborators have demonstrated that ML Cr_2Se_3 on graphene exhibits spin-valley-coupled FM ordering.[1]

A recent first-principles calculation predicted that a combination of broken inversion symmetry, strong spin-orbit coupling, and magnetic exchange interaction with intrinsic out-of-plane magnetization in ML Cr_2Se_3 results in a spontaneous coupling of spin and valley polarization. This leads to a FM semiconductor with anomalous valley Hall effect.[2] However, there have been no experimental reports of spin-valley coupling in either bulk or ML Cr_2Se_3, or in any non-van der Waals material. Furthermore, there is no experimental evidence that magnetic ordering temperatures are enhanced or exceed 55 K due to spin-valley coupling.[3]

Cr_2Se_3 is a non-van der Waals material, and its ML consists of a quintuple set of Se-Cr-Se-Cr-Se atomic layers, as shown in **Fig. 1(a)**. The authors used molecular beam epitaxy to grow 1 to 3 MLs of Cr_2Se_3 on graphene. The reflection high-energy electron diffraction (RHEED) pattern of the fabricated film showed clear streaks associated with the 1 × 1 structure of Cr_2Se_3, besides the 1 × 1

pattern from the 2 ML graphene (**Fig. 1(b)**). The estimated in-plane lattice constant (3.6 Å) supports the formation of the Cr_2Se_3 phase, which was directly confirmed by transmission electron microscopy measurements. The low-energy electron diffraction (LEED) pattern showed sharp six-fold 1 × 1 spots originating from the Cr_2Se_3 films, alongside the 1 × 1 spots of graphene (**Fig. 1(c)**), indicating its high-quality single crystallinity. Soft X-ray photoemission spectroscopy revealed Cr^{3+} features, further supporting the formation of the Cr_2Se_3 phase. To clarify ferromagnetism, temperature(T)-dependent XAS-XMCD measurements of the Cr L-edge (2p–3d) were conducted at the **TLS 11A1** Dragon beamline. The XAS spectrum of 1 ML Cr_2Se_3 at T = 70 K, for both positive and negative out-of-plane magnetic fields (± 1.0 T), showed Cr L_3 and L_2 main peaks at $h\nu$ ~ 577 eV and 585 eV (**Fig. 1(d)**), respectively. The XAS difference spectrum between the +1.0 T and −1.0 T spectra exhibited small but clear features and indicated a finite XMCD, thus proving FM ordering. The authors then performed charge-transfer cluster model spectral calculations, which reproduced the experimental XAS and XMCD spectra (**Fig. 1(d)**). The resulting electronic parameters indicated that 1 ML Cr_2Se_3 is a negative-charge transfer material with a Cr^{3+} $t_{2g}^{3\uparrow}$ electron configuration and a magnetic moment of 3.4 μB per Cr atom. These results establish that 2D magnetism is realized in the non-van der Waals type 1 ML Cr_2Se_3 material.[1]

To estimate T_C from magnetization-sensitive measurements, the authors performed T-dependent XMCD measurements in the total electron yield mode. **Figure 2(a)** shows T-dependent XMCD intensity for 1 ML Cr_2Se_3 at the Cr L_3 and L_2 edges for T = 70, 180, 225, and 250 K. The XMCD intensity systematically reduced from T = 70 K to 225 K, and by T = 250 K, the XMCD signal had vanished. Similarly, the XMCD intensity for 3 ML Cr_2Se_3 at T = 70, 125, 150, and 175 K, as shown in **Fig. 2(b)**, signifies a finite XMCD intensity up to T = 150 K but became negligible at T = 175 K. The XMCD intensity at the L_3 peak ($h\nu$ = 577.0 eV) plotted vs. T in **Fig. 2(c)** suggests that the T_C value from the XMCD measurements is 225–250 K and 150-175 K for 1 and 3 ML, respectively.

The authors also employed T-dependent ARPES with circularly polarized photons to study the relationship between band dispersions and FM ordering, as shown in **Figs. 3(a)–3(c)** on the next page. The results showed that localized Cr $3d^{\uparrow}$-t_{2g} bands exhibit systematic energy shifts and band splitting of spectral features at the Γ, K, and K' points at high binding energies (E_B), and occupancy of the itinerant Cr 3d–e_g valleys at the K and K' points near the Fermi level (E_F). As shown in **Fig. 3(d)**, at the Γ point, a main peak is observed at E_B = 2.16 eV with a shoulder at 2.36 eV at T = 40 K, indicating the existence of a double

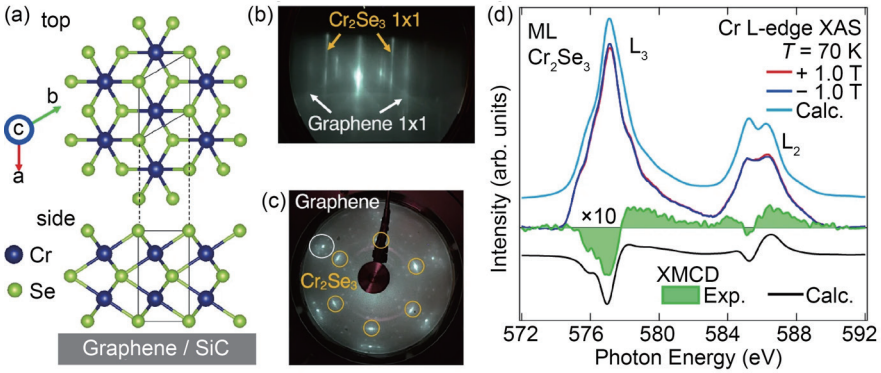

Fig. 1: Fabrication and characterization of ML Cr_2Se_3 film. (a) Top and side views of the crystal structure (P6-m2 space group) of ML Cr_2Se_3 on 2 ML graphene/SiC (0001). Black rectangles indicate the unit cell, which consists of quintuple layers with a Se-Cr-Se-Cr-Se stacking sequence. (b) RHEED pattern of ML Cr_2Se_3. White and yellow arrows indicate the 1 × 1 patterns from graphene and Cr_2Se_3, respectively. (c) LEED pattern of ML Cr_2Se_3 measured with a primary electron energy of 90 eV. Yellow and white circles represent the 1 × 1 spots from Cr_2Se_3 and graphene, respectively. (d) Cr L edge (2p–3d) XAS spectrum of ML Cr_2Se_3 measured with an applied magnetic field of ±1.0 Tesla (T) at 70 K (red and blue curves). The green area shows the difference between +1.0 T and −1.0 T data, expanded vertically by a factor of 10, corresponding to the experimental XMCD. Numerical simulations based on the charge transfer cluster model for XAS and XMCD spectra are shown with light blue and black curves, respectively. [Reproduced from Ref. 1]

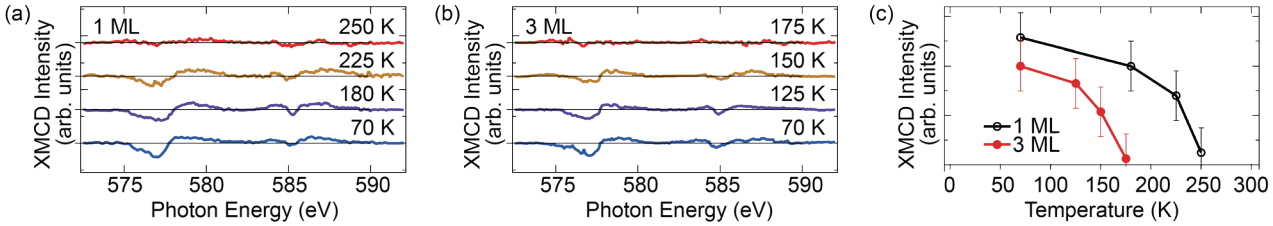

Fig. 2: Determination of T_C by XMCD measurements. (a,b) Temperature dependence of the XMCD signal at the Cr L_3 and L_2 edges for 1 ML and 3 MLs, respectively. (c) Plot of XMCD intensity at the L_3 peak ($h\nu$ = 577.0 eV) versus temperature for 1 ML and 3 MLs, showing a reduction of T_C with increasing number of layers. [Reproduced from Ref. 1]

peak (p1 and p2 in **Fig. 3(d)**). Similar band splitting was also observed at the K/K' point, as shown for the K' point in **Fig. 3(e)**. These band splittings of Cr–Se hybridized states disappear between T = 225–250 K (**Figs. 3(d) and 3(e)**), consistent with T_C ~225 K for 1 ML Cr_2Se_3 estimated from XAS-XMCD (**Fig. 2(a)**).

Evidence for CD in the occupied $t_{2g}{}^{\uparrow}$ bands at the K and K' points at 40 K for ML Cr_2Se_3 was observed, as shown in **Fig. 3(f)**. Using right and left circularly polarized light (C+ and C-), the energy distribution curves (EDCs) obtained at the K point (red and pink curves) showed a difference in peak intensity, indicating finite CD. This CD was also observed at the K' point (blue and light blue curves), but with a sign reversal compared to the K point, as shown by the vertically expanded subtracted EDCs (yellow and purple curves). A sign reversal of CD was also found for the $e_g{}^{\uparrow}$ pockets between the K and K' points (see inset to **Fig. 3(f)**). Notably, the sign is reversed between the $t_{2g}{}^{\uparrow}$ and $e_g{}^{\uparrow}$ bands. These results suggest that photoelectron excitations are asymmetric between the K and K' points, indicating valley-selective CD, *i.e.*, spin-valley polarization. Consequently, the t_{2g}–e_g spin-valley coupling at the K/K' points of the hexagonal Brillouin zone leads to spontaneous FM ordering. The CD observed in ARPES also provided clear evidence of magnetically sensitive spin-valley polarized states.[1]

Finally, the authors confirmed that the reduction of T_C with an increasing number of layers is caused by a decrease in the electron carrier density transferred from the substrate across the Cr_2Se_3:graphene interface. The XAC-XMCD and ARPES results indicate that T_C is proportional to the carrier density (which correlates with the measured spectral density of states at E_F). The results suggest that ferromagnetism is likely due to the localized t_{2g} spins coupled *via* the Ruderman-Kittel-Kasuya-Yosida (RKKY) interaction active in the valley e_g-electron pockets of Cr_2Se_3 films grown on graphene. (Reported by Ashish Chainani)

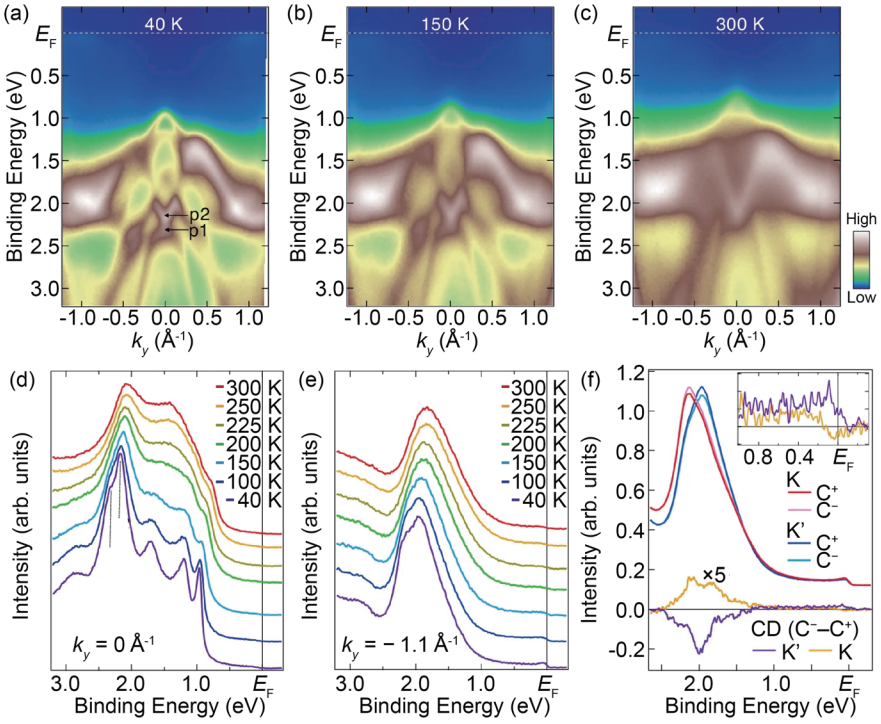

Fig. 3: Temperature evolution of band structure and evidence for spin-valley polarization. (a–c) ARPES intensity plots along the ΓK cut measured at T = 40, 150, and 300 K, respectively, using circularly polarized photons of $h\nu$ = 75 eV. Peaks p1 and p2 are also indicated. (d,e) Temperature dependence of EDCs at selected k cuts along k_y = 0.0 (Γ) − 1.1 Å^{-1} (K'), respectively. (f) EDCs for ML Cr_2Se_3, obtained at the K and K' points with C+ and C- polarized lights using $h\nu$ = 75 eV. Yellow and purple curves represent subtracted EDCs obtained with C+ and C- photons expanded vertically by 5 times. The inset shows the expansion near E_F. A clear CD associated with spin-valley polarization reverses its sign between the K and K' points. [Reproduced from Ref. 1]

This report features the work of Chien-Wen Chuang, Takafumi Sato, Ashish Chainani and their collaborators published in Nat. Commun. ***16****, 3448 (2025).*

TLS 11A1 (Dragon) MCD, XAS

- XAS-XMCD
- Materials Science, Condensed-matter Physics

References

1. C.-W. Chuang, T. Kawakami, K. Sugawara, K. Nakayama, S. Souma, M. Kitamura, K. Amemiya, K. Horiba, H. Kumigashira, G. Kremer, Y. Fagot-Revurat, D. Malterre, C. Bigi, F. Bertran, F. H. Chang, H. J. Lin, C. T. Chen, T. Takahashi, A. Chainani, T. Sato, Nature Comm. **16**, 3448 (2025).
2. Z. He, R. Peng, X. Feng, X. Xu, Y. Dai, B. Huang, Y. Ma, Phys. Rev. B. **104**, 075105 (2021).
3. B. Edwards, O. Dowinton, A. E. Hall, P. A. E. Murgatroyd, S. Buchberger, T. Antonelli, G.-R. Siemann, A. Rajan, E. Abarca Morales, A. Zivanovic, C. Bigi, R. V. Belosludov, C. M. Polley, D. Carbone, D. A. Mayoh, G. Balakrishnan, M. S. Bahramy, P. D. C. King , Nat. Mater. **22**, 459 (2023).